THE COEFFICIENTS OF THERMAL EXPANSION OF WOOD AND WOOD PRODUCTS

Information Reviewed and Reaffirmed

March 1956

No. 1487

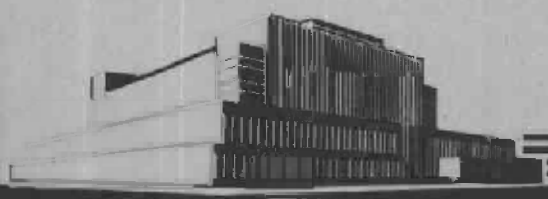

FOREST PRODUCTS LABORATORY
MADISON 5, WISCONSIN

UNITED STATES DEPARTMENT OF AGRICULTURE
FOREST SERVICE
In Cooperation with the University of Wisconsin

THE COEFFICIENTS OF THERMAL EXPANSION OF WOOD AND WOOD PRODUCTS[1]

By

RICHARD C. WEATHERWAX, Chemist
and
ALFRED J. STAMM, Chemist

Forest Products Laboratory,[2] Forest Service
U. S. Department of Agriculture

Introduction

Wood is an anistropic material possessing different coefficients of linear thermal expansion along its radial, tangential, and fiber axes. This anisotropy, modified by the treatments involved, remains a basic property of all the derived structural products of wood, in which the fiber arrangement is not destroyed.

Little data are available on the thermal expansion of natural solid wood, plywood, impreg, compreg, and papreg, and none on staypak, and hydrolyzed wood, plastics and laminated sheets. Consequently, the studies herein reported were made at the Forest Products Laboratory in an effort to obtain such data. The coefficients of linear thermal expansion (hereafter called "α" for brevity) were measured on each of these materials in the three structural directions. The variation of α with specific gravity was determined on a series of 26 solid, oven-dry specimens of 9 different species of untreated wood. The effects of radial compression, resin treating, and cross-banding on the values of α were determined on a series of 23 birch laminates. The values of α for papreg and hydrolyzed-wood plastic were also determined.

General formulas were developed that permit calculation of the coefficients of linear thermal expansion of wood in any grain direction of the specimen

---

[1] Original report published in June 1946.

[2] Maintained at Madison, Wis., in cooperation with the University of Wisconsin.

from the original and final specific gravities, the percentage by weight of resin and glue present, the percentage of cross-banding, and the slope of grain relative to any three axes of reference.

Method of Measurement

The coefficients of linear thermal expansion (α) of each specimen were measured radially, tangentially, and parallel to the fibers over a temperature range of from +50° to -55° C., using specimens 10 centimeters long for measurements in the fiber direction and 1 centimeter long for measurements of transverse directions. The apparatus was a quartz dilatometer of the optical-lever type (fig. 1). The length of the optical lever was 500 centimeters, and the spacing of the mirror legs 0.097428 centimeters. The meter-long convex scale with a radius of curvature equal to the optical lever length (fig. 2) could be adjusted during a run to accommodate an optical lever swing of 176 centimeters. The zero point and lever deflection were read through two telescopes with a magnification of 20x (fig. 3). The apparatus was calibrated against pure annealed silver, pure annealed copper, and calibrated samples of steel and of copper alloy obtained from the National Bureau of Standards. The equations for the thermal expansion of the copper and silver were taken from the International Critical Tables (7). All four samples agreed well, indicating an optical lever magnification of 10,264 ± 6 times. Temperatures were measured with a copper-constantan thermocouple, and type-K potentiometer, calibrated against condensing steam, melting ice, melting mercury and subliming dry ice. The expansion of the dilatometer was calculated from data for quartz taken from the International Critical Tables (8).

The measurements were made in an air bath with a plate glass door in which the temperature was controlled by a thermostat. Anhydrous alumina gel was used as a desiccant within the bath. The temperature was varied by the use of a surrounding alcohol jacket, cooled by circulation through a tank containing dry ice and alcohol, and heated electrically. The complete apparatus is shown in figure 3. Readings of specimen length were taken at +50°, +25°, o°, -25°, -40°, -55°, 0°, and +50° C., to an accuracy of ± 3° C., the complete cycle requiring about 6-1/2 hours. The temperature was maintained constant to ± 0.1° C. for 5 minutes before each reading was made.

The apparatus was mounted on a stone table with the supporting pillars resting on sand beneath the foundation of the building and free from contact with the building, while the air bath was supported by a framework from the floor (fig. 3). Any vibration of the bath was thus prevented from being transmitted to the dilatometer and the specimen.

Natural Solid Wood

The only thermal expansion data for natural wood to find their way into American physical, chemical, and engineering handbooks were obtained by Villari (21) and Glatzel (3) in the previous century. Other data have been obtained by Struve (19), Hendershot (6), and Menzel (11). Menzel is the only one to consider variations in α with the specific gravity of the wood (red oak only) and differences between α_t and α_r (tangentially and radially). He failed to find a definite correlation between his two transverse expansion values and the specific gravity as is obtained in this report. He did, however, find α_t to be significantly greater than α_r, which is in agreement with the findings of this study.

Measurements were made on the following nine species: Sitka spruce (Picea sitchensis), white fir (Abies concolor), Douglas-fir (Pseudotsuga taxifolia), redwood (Sequoia sempervirens), balsa (Ochroma logapus), cottonwood (Populus deltoides), yellow-poplar (Liriodendron tulipifera), yellow birch (Betula lutea), and sugar maple (Acer saccharum), using specimens of low, medium, and high specific gravity for each species except balsa. The samples, 10 by 1 by 1 centimeter in size, were cut from clear wood specimens previously used at the Laboratory for moisture content-shrinkage studies as part of extensive strength investigations (10) (except for balsa).

The experimental data for yellow birch are presented graphically in figure 4. The expansion increases with an increase in temperature slightly more at high than at low temperatures. For this reason both α_{+50} to $_{-55}$ and α_{+55} to $_{0}$ have been calculated and used separately in comparisons. For ordinary use, however, these differences may be neglected. In all cases the descending and ascending temperature changes gave practically identical results; the average variance between the two slopes for all the species and modified wood products was ±0.4 percent.

The α values determined between +50° C. and 0° C. and corrected for the slight variations in slope of grain as shown in appendix A are plotted in figure 5. The values of α in the radial and tangential directions (α_r and α_t) increased in all cases with the specific gravity, but the α values parallel to the fibers ($\alpha_{||}$) were apparently independent of specific gravity and approximately the same for all the species studied. The radial and tangential values of α fall into three groups; Sitka spruce, white fir, Douglas-fir, redwood, cottonwood, and yellow-poplar all have approximately the same α-specific gravity relationship; birch and maple fall into another group with lower values of α than the specific gravity would indicate; while balsa stands alone with considerably larger values of α than would be expected on the basis of

the specific gravity. The redwood and Douglas-fir specimens with the highest specific gravity each gave lower values of $\alpha_{\perp}$ (α_t and α_r, see table of symbols) than would be expected on the basis of the other specimens. The redwood specimen contained some compression wood, which perhaps accounts for the low values of $\alpha_{\perp}$ and the highest values of $\alpha_{\parallel}$ of all the woods. This is characteristic of compression wood in expansion due to swelling. The Douglas-fir specimen with the highest specific gravity showed signs of having been case-hardened in drying, which may have restrained the thermal expansion.

The points in figure 5 are too few to show conclusively whether α varies linearly with specific gravity in the transverse directions. Straight lines through the origin, however, represent the data about as well as any other relationship, except perhaps in the case of balsa.

Table 1 gives the values of α in the three structural directions determined between + 50° C. and -50° C. and between + 50° and 0° C. for each of the nine species with specific gravity values approximately equal to the average for the species. The α values were obtained from figure 5, and a similar figure for the measurements was made between + 50° and -50° C. Straight lines through the origin were drawn through the data for each species separately. The point on the lines corresponding to the average specific gravity of the species was taken from the tables of properties of Markwardt and Wilson (10). The average specific gravity values given in the table thus represent the true average for the large group of specimens from which the specimens of this report were chosen.

Menzel (11) gives average values of α for yellow birch ($\alpha_t = 32.0 \times 10^{-6}$, $\alpha_r = 26.3 \times 10^{-6}$, $\alpha_{\parallel} = 2.0 \times 10^{-6}$ per ° C.) and for yellow-poplar ($\alpha_t = 29.9 \times 10^{-6}$, $\alpha_r = 28.3 \times 10^{-6}$ per ° C.), which are in reasonably good agreement with the values given in table 1. Villari (21) gives values of α for maple ($\alpha_{\perp} = 48.4 \times 10^{-6}$ and $\alpha_{\parallel} = 6.4 \times 10^{-6}$ per ° C.) that are somewhat higher than the values of this report.

Birch Veneer Laminates

A limited amount of data is available on the coefficient of linear thermal expansion of laminated compressed wood. A progress report of the British Forest Products Research Laboratory (14) gives values for synthetic-resin film glue-bonded, parallel-laminated, compressed wood made from rotary-cut birch veneer (Jicwood) of $\alpha_{cr} = 147 \pm 10 \times 10^{-6}$ per ° C. and $\alpha_{ct} = 58 \pm 5 \times 10^{-6}$ per ° C. for material with a specific gravity of 1.25, and $\alpha_{cr} = 157 \pm 8 \times 10^{-6}$ per ° C. and $\alpha_{ct} = 59 \pm 5 \times 10^{-6}$ per ° C. for material with a specific

gravity of 1.35, where α_c is the linear thermal expansion of the laminate and the subscripts r, t, and $\parallel$ indicate the radial (direction of compression) tangential and longitudinal values. Greenhill (4) reported values for parallel-laminated, compressed boxwood, hoop pine, and Australian mountain ash compreg (specific gravities 1.35 to 1.39) of $\alpha_{c\parallel} = 8 \times 10^{-6}$ per ° C., $\alpha_{cr} = 102 \times 10^{-6}$ per ° C., and $\alpha_{ct} = 70 \times 10^{-6}$ per ° C. Turner (20) reports values for low-resin-content, parallel-laminated maple Pregwood of $\alpha_{c\parallel} = 4.7 \times 10^{-6}$ per ° C. and $\alpha_{cr} = 63.5 \times 10^{-6}$ per ° C., and for high-resin-content material of $\alpha_{c\parallel} = 5.9 \times 10^{-6}$ per ° C. and $\alpha_{cr} = 68.7 \times 10^{-6}$ per ° C. Turner's results are in good agreement with the following values, but the other two investigators' results appear high.

Rotary-cut yellow-birch sapwood veneer 1/16 inch thick was used to study the effect of gluing, resin treatment, and compression upon the values of the coefficient of linear thermal expansion. In all cases the treated or untreated veneer in the dry but uncured condition was spread with phenolic resin glue (Resinous Products PR14), conditioned at 30 percent relative humidity, and 80° F., and laminated and cured at 310° F. for 30 minutes under varying pressures. Two series of specimens were made from untreated veneer with glue spreads of 3 to 4 grams per square foot per glue line and 7 to 8 grams per square foot per glue line under different degrees of compression. Two series of specimens were made from resin-treated veneer, using Bakelite BR5995 according to the Forest Products Laboratory procedure (18). In one series the resin content was practically constant and the degree of compression varied, while in the other series the resin content was varied and the degree of compression held reasonably constant. All the laminated specimens were dried at 105° C. and stored over phosphorus pentoxide for periods varying from three months to over a year.

α Parallel to Grain

Table 2 gives the data for the coefficient of linear thermal expansion of the laminates in the fiber direction, $\alpha_{c\parallel}$. The data indicate that there is no significant change in $\alpha_{c\parallel}$ with changes in the degree of compression. The presence of both glue line and treating resin, however, does increase the $\alpha_{c\parallel}$ values. Because of this it seemed worth while to try to express the $\alpha_{c\parallel}$ values in terms of $\alpha_{w\parallel}$ the wood component, and α_R, the total resin-plus-glue component, as acting in parallel combination against each other. The following general equation was derived in Appendix B:

$$\alpha = \frac{E_w \alpha_w (1 - n_s) + E_R \alpha_R n_s}{E_w (1 - n_s) + E_R n_s} \qquad \text{(B-3)}$$

in which E is the modulus of elasticity, and n_s is the fraction of the cross section of the wood-resin system made up of resin-plus-glue component in a plane at right angles to the direction of measurement. E_R and α_R will not vary with the different directions in the wood because of the isotropic nature of the resin. E_w, α_w, and α_c, on the other hand, will vary with the direction of the grain of the wood. Hence, these symbols will have to be followed by subscripts ⊥, t, or r for thermal expansion in the fiber, tangential, and radial directions, respectively.

In using equation (B-3) the experimental fractional resin content, n_R, which is expressed on a weight basis, was converted to n_v on a volume basis by considering the specific gravity of the resin to be 1.28 and of the wood substance to be 1.46. n_s was calculated from n_v by considering the resin to be distributed in a continuous manner in the fiber direction. The fractional length in the fiber direction consisting of resin is thus 1.0 and in the two transverse directions $(n_v)^{1/2}$. Hence, for measurements in the fiber direction $n_s = n_v$ and for measurements in the transverse directions

$$n_s = \frac{(n_v)^{1/2}}{(n_v)^{1/2} + (1 - n_v)^{1/2}}$$

To test equation (B-3) for thermal expansion in the fiber direction, it was solved for E_R, giving

$$E_R = E_{w\perp} \times \frac{(1 - n_s)}{n_s} \times \frac{(\alpha_{w\perp} - \alpha_{c\perp})}{(\alpha_{c\perp} - \alpha_R)} \qquad (1)$$

$E_{w\perp}$ in compression was determined from strength data for birch parallel to the grain by correcting to 0 percent moisture content and extrapolating the modulus of elasticity-specific gravity relationship to a specific gravity of 1.46, that of wood substance, (10, 12), giving $E_{w\perp} = 6.85 \times 10^6$ pounds per square inch. $\alpha_{w\perp} = 3.36 \times 10^{-6}$ per ° C. was taken from table 1 for solid wood. $\alpha_R = 34.48 \times 10^{-6}$ per ° C. was determined experimentally on a bar

of cast treating resin (BR5995) between +50° and -55° C. This value compares favorably with values of 14 to 44 x 10^{-6} per ° C. given by Souder and Hidnert (16) and 25 to 60 x 10^{-6} per ° C. taken from the "Plastics Properties Chart" (13) for phenolic resin. Using these data, the experimental values of α_c and n_R for one of the laminate specimens, and equation (1), E_R was calculated to be 6.18 x 10^5 pounds per square inch. There are no corresponding modulus of elasticity values in compression given for phenolic resin in plastic tables, but the "Plastics Property Chart" for 1944 gives values in tension of 7 to 10 x 10^5 pounds per square inch, which are in good agreement with the calculated values in compression.

Calculated values for $\alpha_{c\perp}$ were obtained for each of the experimental resin contents by substituting the values for $E_{w\perp}$, $\alpha_{w\perp}$, E_R, α_R, and n_s in equation (B-3). These calculated values of $\alpha_{c\perp}$ together with the observed values are given in table 2. The agreement between the two in general is good.

Figure 6 shows the calculated curve for $\alpha_{c\perp}$ versus resin content and the points for the observed values of $\alpha_{c\perp}$.

α Tangential

The coefficient of linear thermal expansion of the laminate in the tangential direction is complicated in that it is dependent upon the original specific gravity of the wood and the specific gravity change due to compression, as well as upon the combined glue and resin content acting in parallel combination against the wood as in the case of $\alpha_{c\perp}$.

In order to separate the effects of resin content and compression, equation (B-3) was solved for α_{wt}, giving:

$$\alpha_{wt} = \alpha_{ct} + \frac{E_R n_s}{E_{wt}(1 - n_s)} (\alpha_{ct} - \alpha_R) \qquad (2)$$

E_R and α_R having the same values as in the case of the expansion parallel to the grain, E_{wt} = 2.93 x 10^5 pounds per square inch was obtained from transverse compressive strength data for birch by correcting to 0 percent moisture content and extrapolating the modulus of elasticity-specific gravity relationship to the specific gravity of wood substance, 1.46 (10, 12).

n_s was calculated from n_R as indicated under the heading α Parallel to Grain. Values of α_{wt} for the compressed wood were calculated from the experimental values of α_{ct}, table 3 using equation (2). Values of α_t for the original untreated and uncompressed veneer were taken from figure 7. The difference between these two values, $\Delta\alpha_{wt}$ is plotted against the increase in specific gravity of the wood portion of the laminates, ΔG, caused by compression (the final specific gravity of the laminate times $(1 - n_R)$ minus the original specific gravity of the resin-free wood). The $\Delta\alpha_{wt}$ values increase rapidly at first with increases in specific gravity, but soon reach a near-optimum value, whereas the $\Delta\alpha_{wt}$ values for normal wood seem to vary linearly with specific gravity over the normal specific gravity range. This can be explained on the basis of the change in cross section of compressed fibers as shown in figure 8. Due to tangential restraint in pressing, the partly circular fibers become more nearly rectangular. Although the fiber-cavity diameter in the radial direction decreases greatly, it is but slightly changed in the tangential direction. An increase in the amount of wood substance effective in causing expansion in the tangential direction occurs primarily as a result of squaring of the rounded fibers, which presumably is greatest in the early stages of compression. The curve levels off rather abruptly when the applied compression in laminating exceeds the elastic limit in compression.

An empirical equation

$$\alpha_{wt} = \alpha_t + \Delta\alpha_{wt} = \alpha_t + \left(12.129 - \frac{0.7726}{\Delta G + 0.0624}\right) \times 10^{-6} \text{ per } ^\circ\text{C.} \quad (3)$$

relating the increase in α_{wt} with the increase in specific gravity ΔG, was derived from the $\Delta\alpha_{wt}$ curve of figure 7 where α_t is the value for the normal uncompressed solid wood obtained from figure 7. Substituting the values of α_{wt} for the laminates with different degrees of compression and the corresponding values of n_s in equation (3-B), calculated values of α_{ct} were obtained. These are given in table 3, together with the observed values. The agreement, in general, is good. Calculated curves for the relationship of α_{ct} to the fractional resin content are plotted in figure 6 for laminates with an original specific gravity of the wood of 0.6 compressed to a specific gravity of 1.2. The plotted points are the calculated points for laminates with the experimental total resin contents, corrected by the difference between the corresponding calculated and observed values of table 3 for compressed laminates.

α Radial

Still greater complications enter into the calculation of α_{cr}. The wood and resin in parallel with each other in the fiber direction in both the glue-line zone of the plies and the portion free from glue will restrain each other in parallel in the same way as was shown to be the case for $\alpha_{c\mu}$ and α_{ct}. In α_{cr}, however, there is the added effect of the plies and the glue lines, which are in series with each other, having different thermal expansion values in the direction of compression. In the simple case where the glue line and wood are discrete and no resin penetrates the wood

$$\alpha_{cr} = \alpha_{wr} (1 - N_g) + \alpha_R N_g \qquad (4)$$

where N_g represents the fractional thickness in the radial direction made up of glue lines, and α_R is the coefficient of linear expansion of the resin, in this case the glue only. In actual practice the glue line is irregular, with irregular penetration of resin from one to several fiber widths deep in each direction, and with almost perfect wood-to-wood contact in places and resin-filled gaps in other places. As the laminating pressure increases, the wood-to-wood contact improves. Under such conditions the data indicate that it is preferable to assume that the glue line consists of glue-impregnated wood rather than assuming the glue line to be discrete glue. For untreated wood equation (4) then becomes:

$$\alpha_{cr} = \alpha_{wr} (1 - N_g) + \frac{\alpha_{wr}E_{wr} (1 - n_g) + \alpha_R E_R n_g}{E_{wr}(1 - n_g) + E_R n_g} \times N_g \qquad (5)$$

where n_g is the fractional cross section of the glue in the glue line. For treated wood:

$$\alpha_{cr} = \frac{\alpha_{wr}E_{wr} (1 - n_b) + \alpha_R E_R n_b}{E_{wr} (1 - n_b) + E_R n_b} \times (1 - N_g) + \frac{\alpha_{wr}E_{wr} (1 - n_g) + \alpha_R E_R n_g}{E_{wr} (1 - n_g) + E_R n_g} \times N_g \qquad (6)$$

where n_g is the fractional cross section of the glue plus resin in the glue line substance and n_b is the fractional cross section of the treating resin within the solid substance of the plies, assuming that the treating resin in the part of the plies constituting glue line is the same as in the bulk of the plies.

A number of microscopic measurements were made to estimate the glue-line thickness considering it the total thickness to which an appreciable amount of glue penetrates. The average value for all the laminates was about 0.018 ± 0.015 centimeter. Multiplying this value by the number of glue lines, N, and dividing by the thickness of the specimen in centimeters, gives the accumulative glue-line thickness per 1-centimeter thickness of specimen and the fraction of the thickness, N_g, made up of glue lines. For untreated wood

$$n_g = \frac{n_a}{n_a + (1 - n_a)N_g} \tag{7}$$

where n_a is the glue content expressed as the fraction of the solid cross section of the laminate.

For treated wood

$$n_g = \frac{n_a + n_b N_g}{n_a + n_b N_g + (1 - n_a - n_b)N_g} \tag{8}$$

Equation (5) was solved for α_{wr}, using the same values of E_R and α_R that were used in calculating $\alpha_{c\perp}$ and α_{ct} $E_{wr} = 4.33 \times 10^5$ pounds per square inch, obtained from compression data in the radial direction corrected to 0 percent moisture content and a specific gravity of 1.46, and experimental values of α_{cr} for the various untreated laminates. These values, expressed as $\Delta\alpha_{wr}$ are plotted in figure 7 together with the values for $\Delta\alpha_{wt}$. The fact that the $\Delta\alpha_{wr}$ curve is much steeper than the $\Delta\alpha_{wt}$ curve is due to the radial compression, which increases the effective amount of wood substance per unit distance in the radial direction much more than in the tangential direction (fig. 8).

An empirical equation was developed for the change in coefficient of thermal expansion of the wood, α_{wr}, as follows

$$\alpha_{wr} = \alpha_r + \Delta\alpha_{wr} = \alpha_r + (45.194 - \frac{1,853}{\Delta G + 0.041}) \times 10^{-6} \text{ per } ^\circ\text{C.} \tag{9}$$

from the curve of figure 7 that shows the relation of $\Delta\alpha_{wr}$ to the change in specific gravity. Substituting these values for α_{wr} in equations (5) and (6),

calculated values for α_{cr} were obtained. These are given in table 4. The agreement between the observed and calculated values again is good. Calculated values for the relation of α_{cr} to the fractional resin content are plotted in figure 6 for laminates with an original specific gravity of the wood of 0.6 compressed to a final specific gravity of 1.2. Again the plotted points are the calculated points for laminates with the experimental total resin contents corrected by the difference between the corresponding calculated and observed values of table 4 for compressed laminates.

Birch Plywood

The coefficient of thermal expansion of plywood in the thickness direction is practically the same as that of parallel-laminated material. This is shown in table 5 where the calculated values for α_{xr} have been obtained for plywood, using the same equations as those developed for parallel-laminated material. The agreement between calculated and observed values in table 4 for parallel laminates and table 5 for plywood in each case is practically identical.

The coefficient of linear thermal expansion of plywood in the sheet directions is, of course, different from that for the parallel laminates because of the restraint of the plies running in the fiber direction upon the cross bands.

The situation, however, is similar to that from which equation (3-B) was derived. By strictly analogous reasoning, the equation

$$\alpha_x = \frac{\alpha_{c\parallel} E_{\parallel} N_{\parallel} + \alpha_{ct} E_t (1 - N_{\parallel})}{E_{\parallel} N_{\parallel} + E_t (1 - N_{\parallel})} \qquad (10)$$

may be derived. In equation (10) $E_{\parallel}$ and E_t are the Young's moduli for the plies parallel to the grain and in the tangential direction, respectively: $N_{\parallel}$ is the fractional thickness of the plywood made up of plies parallel to the face-ply grain; and $\alpha_{c\parallel}$ and α_{ct} are the linear thermal coefficients of the unassembled plies.

The $E_{\parallel}$ and E_t of resin-treated pieces are the sole unknowns in equation (10). They may be calculated, however, using the equations:

$$E_{\parallel} = E_{w\parallel} (1 - n_s) + E_R n_s \qquad (11)$$

and

$$E_t = E_{wt} (1 - n_s) + E_R n_s \qquad (12)$$

where E_w is the handbook value of the modulus of elasticity in compression corrected for moisture content and the observed specific gravities, the other symbols having their usual significance. In equations (11) and (12) the E in compression corresponding to the observed specific gravity is used because, unlike the conditions in the derivation of equation (3-B), the stresses applied are external and equivalent to the stresses applied in the determination of the handbook values. This method of obtaining E is identical with the method used in obtaining the modulus of elasticity of plywood (1).

To test equations (10, 11, 12), the values of $\alpha_{c\parallel}$ and α_{ct} for the individual plies were calculated, using equation (3-B) and then substituted in equation (10). The $E_\parallel$ and E_t values of equation (10) were derived from equations (11) and (12). The basic data used were

$E_R = 6.18 \times 10^5$ pounds per square inch

$E_{w\parallel} = 4.69G \times 10^6$ pounds per square inch (12)

$E_{wt} = 2.01G \times 10^5$ pounds per square inch (10)

$\alpha_{w\parallel} = 3.36 \times 10^{-6}$ per ° C.

The value of α_{wt} was calculated from equation (3). Table 6 shows the calculated and observed values of $\alpha_{x\parallel}$ and α_{xt}. The agreement between the observed and calculated values is qualitative but not quantitative. This is undoubtedly due to the fact that in the derivation of equation (3-B) and (10) no correction for shear was introduced. In equation (3-B) it was not necessary, since the bonds between the two networks of fibers make them effectively one. In equation (10), however, there is undoubtedly some strain along the glue lines, and, further, an effect which might be termed "washboarding" occurs. If a piece of cross-banded plywood is cut smoothly and then heated, an unevenness may be detected in the once smooth cut. This is "washboarding." Figure 9 shows the effect for both heating and cooling.

Due to imperfect restraint, the tangential plies both expand and contract more than they would if restraint at the glue lines continued throughout the thickness of the plies. Observed coefficients of linear thermal expansion in the plane of the plies of plywood should thus always exceed the calculated values. Table

6 shows that this is generally true. Turner's (20) calculated and observed values for α of cross-banded maple compreg show the same trend, although his percentage variation $\Delta\alpha$ is smaller, due possibly to his use of larger samples. Unfortunately, the difference cannot be calculated, so the best that can be said of equation (10) is that it probably represents the linear thermal expansions of the body of large sheets of plywood, but that it fails when expansion at the edges must likewise be considered, as would be necessary for small specimens.

Rotary-Cut Veneer Laminates Other Than Birch

Because of the limited data obtained on the coefficient of linear thermal expansion of Douglas-fir, Sitka spruce, and sugar maple, they cannot be subjected to the same rigorous theoretical analysis as the data for birch laminates. Table 7 gives the experimental values for α_c in the three different structural directions and the coefficient of volumetric thermal expansion β for both impreg and compreg made from these three woods. The values are in reasonably good agreement with those for birch.

Papreg

Two samples of papreg were made from Mitscherlich-base laminating paper impregnated with spirit-soluble phenolic resin BV16526. The resin content was 36.5 percent of the weight of the treated paper. The panels, one parallel-laminated and the other cross-banded, were pressed under a pressure of 250 pounds per square inch at 325° F. for 25 minutes.

The coefficients of the parallel-laminated material, α_c, were determined parallel to the fiber, $\alpha_{c\parallel}$, at right angles to the fiber in the plane of the laminate α_{ct} and at right angles tothe plane of the plies (direction of pressing), α_{cr} and are given in table 8. In the cross-banded material only the coefficient parallel to the face plies in the plane of the plies, $\alpha_{x\parallel}$, and that in the direction of compression, α_{xr}, were determined. The panel on which measurements were made contained 179 sheets so that α_{xt} could exceed $\alpha_{x\parallel}$ by only about 1 percent. Another respect in which the cross-banded papreg differs from plywood made from relatively thick plies is that the phenomenon of "washboarding" illustrated in figure 9 is negligible, as the plies are so thin that unbalanced end effects within the plies are practically prevented.

It is of interest that $\alpha_{c\parallel}$ for parallel-laminated papreg is appreciably larger than $\alpha_{c\perp}$ for birch compreg, whereas α_{ct} for papreg is much smaller than

the corresponding value of α_{ct} for compreg. These differences reflect the lower degree of fiber orientation in the plane of the plies in paper. The same comparison can be made between $\alpha_{x\parallel}$ for cross-banded papreg and cross-banded compreg.

According to the Plastics Properties Chart (13) the average α value for paper plastics, ranging in specific gravity from 1.30 to 1.36 varies from 17 to 25 x 10^{-6} per ° C. This upper limit is in good agreement with the average α value for parallel-laminated and cross-banded papreg in the three structural directions, 28.35 x 10^{-6} per ° C.

Molded Hydrolyzed-Wood Plastic and Hydrolyzed-Wood Sheet

Only one sample each of molded hydrolyzed-wood plastic in bar form and hydrolyzed-wood sheet panel were run. The data are given in table 8. The former material was made from acid-hydrolyzed maple sawdust (5). The product contained 39.3 percent lignin, the soluble to insoluble lignin ratio being 44.2 percent. The molding powder contained 30 percent of Bakelite phenolic resin BR1922. The bar was formed in a mold under a pressure of 4,000 pounds per square inch at 155° C. for 10 minutes. In such a product molded from powder, the physical properties are essentially the same in all directions. Consequently, only one measurement of α was made.

A panel was pressed from parallel-laminated hydrolyzed-gum sheets (5) containing 18 to 20 percent of Bakelite phenolic resin XV16303. The panel was pressed at a pressure of 2,000 pounds per square inch for 10 minutes at 330° F. Unlike the lignin plastic bar, this material was anisotropic, although not to as great an extent as compreg with a similar resin content. The lack of complete fiber orientation in the paper shows up as it did in the papreg, although there is little similarity in the coefficients of the two materials. The α values for the hydrolyzed-wood plastics are given in table 8. Laminated lignin plastics of specific gravity 1.36 to 1.41 are reported in the Plastics Properties Chart of 1944 (13) as having α values of 21 to 24 x 10^{-6} per ° C.

Summary

The coefficients of linear thermal expansion of 9 species of wood of varying specific gravity were determined in the three structural directions. Equations were derived from correcting for variations in the slope of the grain. $\alpha_{\parallel}$ was shown to be independent of specific gravity; α_t and α_r were shown to vary approximately as the first power of the specific gravity.

The coefficients of linear thermal expansion of resin-bonded birch laminates, both with and without phenolic resin within the cell-wall structure and compressed to various degrees were determined in the three structural directions. Theoretical equations involving the α values for the wood and for the resin and the values of the modulus of elasticity in compression for the wood and the resin were developed from which the α values for the laminates may be calculated. Empirical equations for the effect of increased specific gravity due to compression were developed, which, when used in conjunction with the resin-content equations, make it possible to calculate the α values for compressed resin-treated wood. The agreement between the calculated and the observed values was good.

Equations were developed for calculating the α values for birch plywood and cross-banded resin-treated birch, either uncompressed or compressed. The agreement between the calculated and the observed values was good in the thickness direction, but only qualitative in the sheet direction. This was probably due to shear effects and an edge washboarding effect caused by unbalanced restraint at the ends of the plies.

Data were also obtained for the α values of Douglas-fir, Sitka spruce, and sugar maple impreg and compreg laminates, parallel-laminated and cross-banded papreg, molded hydrolyzed-wood plastic, and hydrolyzed-wood sheet laminates.

Appendix A

Nonaxial Coefficients of Linear Thermal Expansion

Specimens of wood are seldom cut so that their faces are truly in the axial direction of the fiber and parallel and perpendicular to the annual rings. It is thus desirable to be able to calculate the coefficients of linear thermal expansion from data for specimens that do not have their faces in the three structural planes.

Considering first the simplest case of a rectangular wooden block with the grain sloping in only one plane with respect to the faces of the block, such a plane rectangle of wood does not expand into a larger rectangle but becomes a parallelogram of larger area than the original rectangle.

In figure 10 the broken line parallelogram represents the shape of the wood block after thermal expansion from the solid-line rectangle. The grain angle before expansion was θ, and after expansion ϕ. Every point on the broken-line parallelogram corresponds to a point on the rectangle. The relationships are:

$$y_p = y_r\ (1 + dy_r) \tag{1-A}$$

$$x_p = x_r\ (1 + dx_r) \tag{2-A}$$

where the subscripts p and r designate parallelogram and rectangle, respectively.

The linear expansion of the figure may be determined by obtaining the vertical distance between the lines of the rectangle and between the lines of the parallelogram. The equation of the lines may be obtained by substituting in the general equation for a straight line:

$$y - y_1 = m(x - x_1) \tag{3-A}$$

the value of the slope and the coordinates of one point.

The slope of lines ab and cd is tan θ; the slope of the lines ac and bd is -cot θ. Then using the points of intersection of the rectangle and the coordinate axes, the equations are as follows:

$$\text{Line ab;}\quad y = x \tan\theta + \frac{1}{2} g_o \tag{4-A}$$

$$\text{Line cd;}\quad y = x \tan\theta - \frac{1}{2} g_o \tag{5-A}$$

$$\text{Line ac;}\quad y = -x \cot\theta - \frac{1}{2} h_o \cot\theta \tag{6-A}$$

$$\text{Line bd;}\quad y = -x \cot\theta + \frac{1}{2} h_o \cot\theta \tag{7-A}$$

Making use of the transformation equations (1-A) and (2-A), it is possible to transform these equations for the lines ab, ... into the equations for the lines a'b' ..... The transformed equations are as follows:

$$\text{Line a'b';}\quad \frac{y}{1 + \alpha_{\parallel}} = \frac{x}{1 + \alpha_{\perp}} \tan\theta + \frac{1}{2} g_o \tag{8-A}$$

$$\text{Line c'd';}\quad \frac{y}{1 + \alpha_{\parallel}} = \frac{x}{1 + \alpha_{\perp}} \tan\theta - \frac{1}{2} g_o \tag{9-A}$$

$$\text{Line } a'c'; \quad \frac{y}{1+\alpha_{\parallel}} = -\frac{x}{1+\alpha_{\perp}} \cot\theta - \frac{1}{2} h_o \cot\theta \qquad (10\text{-A})$$

$$\text{Line } b'd'; \quad \frac{y}{1+\alpha_{\parallel}} = -\frac{x}{1+\alpha_{\perp}} \cot\theta + \frac{1}{2} h_o \cot\theta \qquad (11\text{-A})$$

where dy_r and dx_r the true coefficients of linear thermal expansion have been termed $\alpha_{\parallel}$ and $\alpha_{\perp}$ respectively. The perpendicular distance between the lines a' b' and c' d' is given by the expression

$$d = \frac{g_o (1+\alpha_{\parallel})}{\sqrt{1 + \frac{(1+\alpha_{\parallel})^2}{(1+a_{\perp})^2} \tan^2\theta}} \qquad (12\text{-A})$$

Figure 10 shows d in equation (12-A) is $g_1 (1 + dg_1)$; but dg_1 is $\alpha_{\perp o}$, so it is possible to write

$$g_1 (1+\alpha_{\perp o}) = \frac{g_o (1+\alpha_{\parallel})}{\sqrt{1 + \frac{(1+\alpha_{\parallel})^2}{(1+\alpha_{\perp})^2} \tan^2\theta}} \qquad (13\text{-A})$$

From figure 10, $g_1 = g_o \cos\theta$; so

$$1 + \alpha_{\perp o} = \frac{(1+\alpha_{\parallel})(1+\alpha_{\perp})}{\sqrt{(1+\alpha_{\parallel})^2 \sin^2\theta + (1+\alpha_{\perp})^2 \cos^2\theta}} \qquad (14\text{-A})$$

Equation (14-A) is eliptical in form, showing that $1 + \alpha_{\perp o}$ increases with increase in θ until it becomes $1 + \alpha_{\perp}$. A strictly analogous series of steps yields the companion equation:

$$1 + \alpha_{\perp o} = \frac{(1+\alpha_{\perp})(1+\alpha_{\parallel})}{\sqrt{(1+\alpha_{\perp})^2 \sin^2\theta + (1+\alpha_{\parallel})^2 \cos^2\theta}} \qquad (15\text{-A})$$

In equations (8-A) through (15-A) lack of the subscript "o" indicates true coefficients of linear thermal expansion, and the inclusion of subscript "o" indicates observed coefficients of linear thermal expansion.

While equations (14-A) and (15-A) give correct values of $\alpha_{\parallel o}$ the magnitude of the α makes numerical computation extremely difficult. Consequently, equation (14-A) was simplified by the following steps: $1 + \alpha_{\perp}$ was reintroduced into the square root, the square root simplified trigonometrically, and then both sides of the equation squared. The resultant equation was cleared of fractions and expanded, yielding an expression of fourth degree in α. The largest α measured in solid specimens is approximately 40×10^{-6} per ° C. Then elimination of a second degree term in α would result in an error of 0.004 percent, which is negligible. Consequently, all second third, and fourth degree terms were eliminated, yielding the expression:

$$\alpha_{\parallel o} = \alpha_{\parallel} \cos^2 \theta + \alpha_{\perp} \sin^2 \theta \qquad (16\text{-A})$$

and by an analogous series of operations:

$$\alpha_{\perp o} = \alpha_{\perp} \cos^2 \theta + \alpha_{\parallel} \sin^2 \theta \qquad (17\text{-A})$$

Equations (16-A) and (17-A) are easy to use and also accurate within the experimental error of any measurements of α. Equations identical with (16-A) and (17-A), except for shear terms on the right side, have been derived from stress-strain relations in wood by March (9). In solid wood specimens, however, the shear terms drop out, thus confirming the correctness of equations (16-A) and (17-A). The steps between (14-A) and (16-A) were not shown, since they are simple algebra and trigonometry. Equations (16-A) and (17-A) express observed α in terms of the true α. Simultaneous solution of equations (16-A) and (17-A) yields the more usable form.

$$\alpha_{\parallel} = \frac{\alpha_{\parallel o} \cos^2 \theta - \alpha_{\perp o} \sin^2 \theta}{\cos 2\theta} \qquad (18\text{-A})$$

and

$$\alpha_{\perp} = \frac{\alpha_{\perp o} \cos^2 \theta - \alpha_{\parallel o} \sin^2 \theta}{\cos 2\theta} \qquad (19\text{-A})$$

These equations hold at any value of θ except 45°. For $\theta = 45°$ an equation involving shearing relative to the axes parallel and perpendicular to the sides of the rectangle must be used.

Figure 11 shows the three simple cases of grain slope in solid blocks of wood. For figure 11A, $\theta = 0 = \epsilon$ and equations (18-A) and (19-A) become:

I

$$\alpha_{\shortparallel} = \frac{\alpha_{\shortparallel} \cos^2 \phi - \alpha_{ro} \sin^2 \phi}{\cos 2\phi} \qquad (20\text{-A})$$

$$\alpha_r = \frac{\alpha_{ro} \cos^2 \phi - \alpha_{\shortparallel o} \sin^2 \phi}{\cos 2\phi} \qquad (21\text{-A})$$

In figure 11B, $\phi = 0 = \epsilon$, and equations (18-A) and (19-A) become:

II

$$\alpha_t = \frac{\alpha_{to} \cos^2 \phi - \alpha_{ro} \sin^2 \theta}{\cos 2\theta} \qquad (22\text{-A})$$

$$\alpha_r = \frac{\alpha_{ro} \cos^2 \theta - \alpha_{to} \sin^2 \theta}{\cos 2\theta} \qquad (23\text{-A})$$

For figure 11C, $\phi = 0 = \theta$, and equations (18-A) and (19-A) become:

III

$$\alpha_{\shortparallel} = \frac{\alpha_{\shortparallel o} \cos^2 \epsilon - \alpha_{to} \sin^2 \epsilon}{\cos 2\epsilon} \qquad (24\text{-A})$$

$$\alpha_t = \frac{\alpha_{to} \cos^2 \epsilon - \alpha_{\shortparallel o} \sin^2 \epsilon}{\cos 2\epsilon} \qquad (25\text{-A})$$

Equations (20-A) through (25-A) were adequate if the grain was at an angle to any one plane of the block, but on some samples the grain may be at angle to two or three planes of the block. Consequently, investigation of these more complicated cases was necessary.

The most complicated case arises when the grain is inclined to each of the planes of the rectangular block. The case is illustrated by figure 12. The

line CA is a wood fiber lying in the radial plane ACD and the tangential plane ACF, and λ, γ, and Ψ are angles measured on the face of the block. The equations of transformation for the coefficients of linear thermal expansion for this case will not be derived in this brief report. The reader interested in their derivation should refer to the report by March (9). The x-, y-, and z- axes in figure 12 are taken to be the natural axes of the wood in the fiber, tangential, and radial directions respectively. The ξ-, η-, and ζ- axes are taken to be the edges of the rectangular block with the origin of both systems of axes at A. Denote $C_{\xi x}$, $C_{\eta x}$, $C_{\zeta x}$ the direction cosines of the x-axis with respect to the ξ-, η-, and ζ-axes, and by similar symbols the direction cosines of the y- and z-axes. Then it follows that

$$\alpha_{\perp o} = \alpha_{\perp} C_{\xi x}^{2} + \alpha_{t} C_{\xi y}^{2} + \alpha_{r} C_{\xi z}^{2} \qquad (26\text{-A})$$

$$\alpha_{to} = \alpha_{\perp} C_{\eta x}^{2} + \alpha_{t} C_{\eta y}^{2} + \alpha_{r} C_{\eta z}^{2} \qquad (27\text{-A})$$

$$\alpha_{ro} = \alpha_{\perp} C_{\zeta x}^{2} + \alpha_{t} C_{\zeta y}^{2} + \alpha_{r} C_{\zeta z}^{2} \qquad (28\text{-A})$$

where the direction cosines are given in the following table ($C_{\xi x} = \cos\phi \cos\theta \cos\Psi + \sin\phi \sin\Psi$, etc.):

	x	y	z
ξ	$\cos\phi \cos\theta \cos\Psi + \sin\phi \sin\Psi$	$-\sin\phi \cos\theta \cos\Psi + \cos\theta \sin\Psi$	$-\sin\theta \cos\Psi$
η	$-\cos\phi \cos\theta \sin\Psi + \sin\phi \cos\Psi$	$\sin\phi \cos\theta \cos\Psi + \cos\phi \cos\Psi$	$\sin\theta \sin\Psi$
ζ	$\cos\phi \sin\theta$	$-\sin\phi \sin\theta$	$\cos\theta$

where

$$\sin\phi = \frac{\cot\gamma}{\sqrt{\cos^2\theta + \cot^2\gamma}} \qquad (29\text{-A})$$

$$\cos\phi = \frac{\cos\theta}{\sqrt{\cos^2\theta + \cot^2\gamma}} \qquad (30\text{-A})$$

$$\sin\theta = \frac{\tan\lambda}{\sqrt{\cos^2\Psi + \tan^2\lambda}} \tag{31-A}$$

$$\cos\theta = \frac{\cos\Psi}{\sqrt{\cos^2\Psi + \tan^2\lambda}} \tag{32-A}$$

Solving equations (26-A), (27-A), (28-A) for $\alpha_{\perp\perp}$, α_t, α_r, it follows that

IV

$$\alpha_{\perp\perp} = \frac{1}{\Delta}\left[\alpha_{\perp\perp o}(C_{\eta y}^2 C_{\zeta z}^2 - C_{\eta z}^2 C_{\zeta y}^2) + \alpha_{to}(C_{\xi z}^2 C_{\zeta y}^2 - C_{\xi y}^2 C_{\zeta z}^2) + \alpha_{ro}(C_{\xi y}^2 C_{\eta z}^2 - C_{\eta y}^2 C_{\xi z}^2)\right] \tag{33-A}$$

$$\alpha_t = \frac{1}{\Delta}\left[\alpha_{\perp\perp o}(C_{\eta z}^2 C_{\zeta x}^2 - C_{\eta x}^2 C_{\zeta z}^2) + \alpha_{to}(C_{\xi x}^2 C_{\zeta z}^2 - C_{\zeta x}^2 C_{\xi z}^2) + \alpha_{ro}(C_{\eta x}^2 C_{\xi z}^2 - C_{\xi x}^2 C_{\eta z}^2)\right] \tag{34-A}$$

$$\alpha_r = \frac{1}{\Delta}\left[\alpha_{\perp\perp o}(C_{\eta x}^2 C_{\zeta y}^2 - C_{\zeta x}^2 C_{\eta y}^2) + \alpha_{to}(C_{\zeta x}^2 C_{\xi y}^2 - C_{\xi x}^2 C_{\zeta y}^2) + \alpha_{ro}(C_{\xi x}^2 C_{\eta y}^2 - C_{\eta x}^2 C_{\xi y}^2)\right] \tag{35-A}$$

where

$$\Delta = C_{\xi x}^2(C_{\eta y}^2 C_{\zeta z}^2 - C_{\zeta y}^2 C_{\eta z}^2) + C_{\eta x}^2(C_{\xi z}^2 C_{\zeta y}^2 - C_{\xi y}^2 C_{\zeta z}^2) + C_{\zeta x}^2(C_{\xi y}^2 C_{\eta z}^2 - C_{\xi z}^2 C_{\eta y}^2) \tag{36-A}$$

These equations, I through IV relating the true and observed α with the grain angle, were applied to all the solid wood samples. The percentage change in α_t and α_r in all cases is small, but in some instances the percentage change in $\alpha_{\perp\perp}$ is large.

Appendix B

For the purpose of developing a formula relating α and resin content, a piece of resin-treated wood was regarded as two intimately intermeshed fibrous lattices, with the normal fiber structure of the wood as one lattice, and the enveloping resin as the second parallel lattice. The two lattices were considered to be joined continuously along their surfaces of contact so that a strain on one lattice is, perforce, that on the other. Under such conditions the expansion of the composite lattice must be a function of (1) the relative amounts of each material present, (2) the Young's moduli of the two materials, (3) the thermal stress acting on each, and (4) the α of each material taken separately.

Due to the fact that α_R for the resin is greater than α_w for the wood, increasing the temperature produces compression in the resin and tension in the wood. Assume that the resin is acted on by a compressive force f necessary to compress the parallel resin lattice by an amount $(\alpha_R - \alpha_c)\,\Delta T$. Then

$$f = E_R\, n_s\, A\, (\alpha_R - \alpha_c)\Delta T \qquad \text{(B-1)}$$

where n_s is the fractional solid cross-section occupied by resin in a plane at right angles to the direction of measurement within the composite lattice, α_c is the α of the parallel-laminated combined wood-resin lattice, A is the cross-sectional solid area of the combined lattice, E_R is the Young's modulus of the resin, and ΔT is the temperature change in degrees centigrade. The unit elongations of the wood and resin must be equal.

Hence,

$$\alpha_w \Delta T + \frac{f}{E_w(1 - n_s)A} = \alpha_R \Delta T - \frac{f}{E_R\, n_s\, A} \qquad \text{(B-2)}$$

Substituting equation (B-1) in equation (B-2) and solving for α_c, it is found that

$$\alpha_c = \frac{E_w\, \alpha_w (1 - n_s) + E_R\, n_s\, \alpha_R}{E_w\,(1 - n_s) + E_R\, n_s} \qquad \text{(B-3)}$$

E_R in equation (B-3) is the E_R in compression found in any table of Bakelite resin properties. E_w demands a word of explanation. In the derivation, each lattice is considered as acting against the other. Therefore the E_w must be that of the individual fibers that carry the load. Consequently, E_w as found

in strength tables must be extrapolated to the specific gravity of wood substance, 1.46 (18). Turner (20) developed a similar equation for calculating the coefficient of linear thermal expansion of resin-metal, and similar material, for use as protective coatings on aircraft surfaces.

Symbols

α = coefficient of linear thermal expansion

α_o = α uncorrected where slope of grain exists

$\alpha_{\parallel}$ = α in fiber direction of solid wood

$\alpha_{\perp}$ = α in transverse directions of solid wood

α_c = α of parallel-laminated combined wood-resin-compression systems

α_t = α in tangential direction of solid wood

α_r = α in radial direction of solid wood

α_w = α of wood alone in wood-resin and/or glue systems

α_R = α of resin plus glue in wood-resin systems

α_x = α of plywood
(Combinations of $\parallel$, t, or r with w, c, or x indicate directions of measurement in these systems)

β = coefficient of volumetric thermal expansion

Δ = increment sign

ϵ = angle of grain to radial plane of block

ϕ = angle of grain to tangential plane of block

γ = angle of tangential diagonal to radial plane of block - ϵ

θ = angle of annual rings to tangential plane of block

ξ = axis of rectangular wood block as designated in figure 12

η = axis of rectangular wood block as designated in figure 12

ζ = axis of rectangular wood block as designated in figure 12

A = solid cross section area of wood plus resin

d = differential sign

E = modulus of elasticity (subscripts have same meaning as for α)

f = compressive force necessary to compress parallel resin lattice by an amount $(\alpha_R - \alpha_c)\,\Delta t$

G = specific gravity of wood

g = dimensions of block in y direction

h = dimensions of block in x direction

n_a = fraction of solid cross section of laminate consisting of glue

n_b = fraction of solid cross section of laminate consisting of treating resin

n_R = weight fraction of glue plus resin in laminates

n_s = fraction of solid cross section of laminate consisting of glue plus resin

n_g = fraction of solid cross section of glue line consisting of glue plus resin

N = number of glue lines per specimen

N_g = thickness fraction of combined glue lines relative to total thickness of laminate

$N_{\perp\perp}$ = thickness fraction of the plies of plywood with the grain of the plies parallel to the direction of measurement of property

T = temperature in degrees Centigrade

x = axis of wood block

y = axis of wood block

z = axis of wood block

References

1. ANC Handbook on the Design of Wood Aircraft Structures, Article 2.52, p. 27 (1942).

2. Clash, R. F., and Rynkiewicz, L. M. Ind. Eng. Chem. 36:279 (1944).

3. Glatzel, P. Ann. de Physik und Chemie 160:497-514 (1877).

4. Greenhill, W. L. Council for Sci. and Ind. Res., Australia, "Physical Properties of Improved Woods," Progress Report 4. (1944).

5. Guss, C. O. "Acid Hydrolysis of Waste Wood for Use in Plastics," Forest Products Laboratory Report No. R1481, (June 1945) Out of Print.

6. Hendershot, O. P. Science 60:456-7 (1924).

7. International Critical Tables, II:460-2 (1926), 1st ed. McGraw-Hill Book Co., New York.

8. Ibid., IV:21 (1926).

9. March, H. W., "Stress-Strain Relations in Wood and Plywood Considered as Orthotropic Materials." Forest Products Laboratory Report No. 1503, February 1944, Information Reviewed and Reaffirmed March 1956.

10. Markwardt, L. J., and Wilson, T. R. C., "Strength and Related Properties of Woods Grown in the United States." U.S.D.A. Tech. Bul. 479 (1935), pp. 35, 37, 51.

11. Menzel, C. A. U. S. Dept. Agric. Wood Handbook, table 3, p. 43, (1955).

12. Newlin, J. A., and Wilson, T. R. C., "Relationship of Shrinkage and Strength Properties of Wood to Its Specific Gravity," U. S. Dept. Agric. Bul. 676 (1919).

13. Plastic Properties Chart - 1944. Industrial Magazine Service, Inc., New York.

14. Princes Risborough Forest Products Laboratory, "Moisture and Physical Relations of Composite Wood Products," Progress Report 6, part 1. (1942).

15. Running, T. R., "Empirical Formulas," John Wiley and Sons, Inc., New York, pp. 53-56. (1917).

16. Souder, W. N., and Hidnert, Peter. Bureau of Standards Sci. Papers No. 352 (1919).

17. Stamm, A. J., and Hansen, L. A. J. Phys. Chem. 41:1007 (1937).

18. Stamm, A. J., and Seborg, R. M., Forest Products Laboratory Report No. 1380 Revised (1943), and No. 1381 Revised (1944).

19. Struve, W. Fortschrette der Physik 6:48-52 (1850).

20. Turner, P. S. NACA, "Report on the Problem of Thermal Expansion Stresses in Reinforced Plastics," June 1942.

21. Villari, E. Annales de Chemie et de Physique 14:503 (1868).

22. Wiley, F. E. Ind. Eng. Chem. 34:1052-56 (1942).

Table 1.--Average coefficients of linear thermal expansion per ° C. of nine species of solid wood over two different temperature ranges for the average specific gravity of the species

Species	Average specific gravity[1]	$\alpha_t \times 10^6$		$\alpha_r \times 10^6$		$\alpha_{\parallel} \times 10^6$	
		+50° to -50° C.	+50° to 0° C.	+50° to -50° C.	+50° to 0° C.	+50° to -50° C.	+50° to 0° C.
Yellow birch	0.66	38.3	39.4	30.7	32.2	3.36	3.57
Sugar maple	.68	35.3	37.6	26.8	28.4	3.82	4.16
Yellow-poplar	.43	29.7	31.4	27.8	27.2	3.17	3.55
Cottonwood	.43	32.6	33.9	23.2	23.3	2.89	3.17
Balsa	.17[2]	.....	24.1	.....	16.3	.....	.....
Douglas-fir[3]	.51	42.7	45.0	27.9	27.1	3.16	3.52
Sitka spruce	.42	32.3	34.6	23.8	23.9	3.15	3.50
White fir	.40	32.6	31.6	21.8	21.7	3.34	3.90
Redwood[3]	.42	35.1	35.8	23.6	23.9	4.28	4.59

[1] Average specific gravity (based on weight and volume when oven dry) taken from tables of properties given by Markwardt and Wilson (10) for specimens from which the test specimens of this report were chosen.

[2] Specific gravity average of values for two specimens tested.

[3] Low transverse values of α for highest specific gravity specimen were omitted.

Table 2.--Coefficients of linear thermal expansion of rotary-cut birch laminates in the fiber direction, $\alpha_{c\parallel}$ with different resin contents and degrees of compression

Specific gravity of product	Resin + glue content, n_R	$\alpha_{c\parallel} \times 10^6$		Error
		Observed	Calculated	
	Fraction of total weight	Per ° C.	Per ° C.	Percent
0.722	0.031	3.25	3.46	+6.45
.962	.049	3.67	3.52	-4.08
1.170	.047	3.62	3.52	-2.76
1.279	.047	3.41	3.52	+3.22
.866	.332	4.65	4.87	+4.73
1.205	.335	4.90	4.89	-.20
1.344	.341	4.97	4.93	-.80
1.158	.040	3.21	3.49	+8.71
1.305	.248	4.25	4.38	+3.06
1.310	.335	5.16	4.89	-5.23
1.323	.340	5.17	4.93	-4.65
1.308	.343	4.93	4.95	+.41
1.249	.370	4.86	5.13	+5.55
			Average.....	±3.83

[1] Disregarding sign.

Table 3.--Coefficients of linear thermal expansion of rotary-cut birch laminates at right angles to the fiber direction in the plane of the plies, α_{ct} with different resin contents and degrees of compression

Number of glue lines, N	Specific gravity: Original untreated wood	Specific gravity: Final product	Glue content	Resin + glue content, n_R	$\alpha_{ct} \times 10^6$: Observed	$\alpha_{ct} \times 10^6$: Calculated	Error
			Fraction of total weight	Fraction of total weight	Per ° C.	Per ° C.	Percent
5	0.697	0.722	0.031	0.031	40.29	40.00	-0.72
8	.553	.945	.049	.049	38.01	40.42	+6.43
13	.493	1.178	.047	.047	38.99	38.49	-1.28
13	.493	1.298	.047	.047	37.88	38.59	+1.87
6	.621	.678	.085	.085	35.42	35.97	+1.55
8	.648	.793	.073	.073	42.20	41.44	-1.81
11	.643	1.050	.083	.083	44.35	42.99	-3.07
14	.656	1.364	.089	.089	45.73	43.52	-4.84
5	.545	.856	.006	.332	35.11	35.34	+.65
8	.613	1.305	.009	.335	39.24	39.05	-.48
13	.613	1.346	.015	.341	38.64	39.05	+1.06
11	.538	1.169	.040	.040	40.21	40.26	+.12
11	.600	1.305	.018	.248	39.47	39.44	-.08
11	.582	1.310	.013	.335	43.08	38.42	-10.80
11	.577	1.323	.013	.340	38.64	38.24	-1.03
11	.583	1.308	.013	.343	39.32	38.34	-2.50
11	.567	1.249	.013	.370	37.65	37.64	-.30
						Average	±1.67

[1] Disregarding sign.

Table 4.--Coefficients of linear thermal expansion of rotary-cut birch laminates in the direction of pressing, α_{cr}, with different resin contents and degrees of compression

Number of glue lines, N	Total glue line thickness N_g	Specific gravity: Original untreated wood	Specific gravity: Final product	Glue content	Resin content	Glue + resin content of glue line, n_g	$\alpha_{cr} \times 10^6$: Observed	$\alpha_{cr} \times 10^6$: Calculated	Error
	Fraction of total thickness			Fraction of total weight of wood	Fraction of total weight of wood	Fraction of cross section of glue line	Per ° C.	Per ° C.	Percent
5	0.096	0.697	0.722	0.031	0.0	0.660	36.64	36.92	+0.76
8	.150	.553	.945	.049	.0	.620	63.64	64.57	+1.46
13	.240	.493	1.178	.047	.0	.482	62.76	62.63	-.21
13	.237	.493	1.298	.047	.0	.487	65.34	63.00	-3.59
6	.136	.610	.678	.085	.0	.705	35.00	31.54	-9.85
8	.119	.648	.793	.073	.0	.716	57.18	60.35	+5.52
11	.163	.643	1.050	.083	.0	.662	68.91	67.76	-1.67
14	.204	.656	1.364	.089	.0	.626	60.17	69.17	+14.95
5	.094	.545	.856	.006	.326	.673	37.05	41.83	+12.91
8	.148	.613	1.305	.009	.326	.643	55.20	50.50	-8.50
13	.239	.613	1.346	.015	.326	.649	55.58	49.97	-10.10
11	.208	.538	1.169	.040	.0	.464	63.44	65.21	+2.80
11	.209	.600	1.305	.018	.230	.657	59.14	52.09	-11.92
11	.215	.582	1.310	.013	.322	.634	54.23	49.73	-8.30
11	.218	.577	1.323	.013	.327	.647	55.69	49.57	-11.00
11	.214	.583	1.308	.013	.330	.650	54.83	49.43	-9.88
11	.209	.567	1.249	.013	.357	.662	48.41	47.92	-1.01
								Average...	±6.71

[1] Disregarding sign.

Table 5.--Coefficients of linear thermal expansion of rotary-cut birch plywood in the direction of pressing, α_r, with different resin contents and degrees of compression

Number of glue lines, N	Total glue line thickness, N_g	Specific gravity: Original untreated wood	Specific gravity: Final product	Glue content	Resin content	Glue + resin content of glue line, n_g	$\alpha_r \times 10^6$: Observed	$\alpha_r \times 10^6$: Calculated	Error
	Fraction of total thickness			Fraction of total weight of wood	Fraction of total weight of wood	Fraction of cross section of glue line	Per ° C.	Per ° C.	Percent
4	0.098	0.698	0.776	0.031	0.0	0.660	50.77	57.42	+13.10
8	.149	.572	.948	.043	.0	.598	64.51	65.50	+1.53
10	.199	.578	1.185	.046	.0	.527	67.10	66.60	-.74
4	.090	.525	.850	.022	.326	.808	35.78	38.68	+8.10
8	.160	.740	1.302	.020	.326	.728	55.54	50.05	-9.88
8	.170	.589	1.330	.023	.326	.734	58.66	49.52	-15.60
								Average....	[1]8.15

[1] Disregarding sign.

Table 6.--Coefficient of linear thermal expansion of rotary-cut birch plywood in the plane of the plies with different resin contents and degrees of compression

Number of glue lines, N	Specific gravity: Original untreated wood	Specific gravity: Final product	Resin + glue content, n_R	$\alpha_{x\parallel} \times 10^6$: Observed	$\alpha_{x\parallel} \times 10^6$: Calculated	$\alpha_{x\parallel} \times 10^6$: Error	$\alpha_{xt} \times 10^6$: Observed	$\alpha_{xt} \times 10^6$: Calculated	$\alpha_{xt} \times 10^6$: Error
			Fraction of total weight	Per ° C.	Per ° C.	Percent	Per ° C.	Per ° C.	Percent
2	0.698	0.776	0.027	5.29	4.68	-11.5			
4	.698	.776	.031	5.71	5.13	-10.1	7.61	7.03	-7.6
8	.572	.948	.043	6.72	5.31	-21.0	7.02	6.28	-10.5
10	.578	1.090	.046	6.99	5.35	-23.5	7.18	6.09	-15.2
10	.612	1.185	.046	7.16	5.36	-25.1	7.84	6.11	-22.0
4	.525	.850	.348	6.74	7.44	+10.4	9.85	10.01	+1.6
8	.740	1.302	.346	8.84	7.70	-12.9	9.10	9.10	+0.0
8	.589	1.333	.349	8.73	7.49	-14.2	9.25	8.78	-5.1

Table 7.--Coefficients of linear and cubical thermal expansion of Douglas-fir, Sitka spruce, and sugar maple impreg and compreg

Species	Specific gravity of product	n_R	$\alpha_{c\perp} \times 10^6$	$\alpha_{ct} \times 10^6$	$\alpha_{cr} \times 10^6$	$\beta \times 10^6$
		Per ° C.	Per ° C.	Per ° C.	Per ° C.	Per ° C.
Douglas-fir	0.880	0.310	5.95	32.52	42.89	81.36
	.506	.322	5.46	31.20	21.34	58.00
Sitka spruce	.972	.338	4.05	33.36	45.20	82.61
	.565	.310	4.74	30.89	24.38	60.01
Sugar maple	1.347	.342	5.31	42.26	55.09	102.66
	.987	.361	5.42	36.57	37.23	79.22

Table 8.--Coefficients of linear thermal expansion per degree Centigrade of wood, hydrolyzed wood, and paper products

Material[1]	Specific gravity of product	Glue + resin content[2]	Linear expansion per ° C. x 10^6			Cubical expansion per ° C. x 10^6
			Fiber or machine direction	Perpendicular to fiber or machine direction in plane of laminations	Pressing direction	
		Percent				
Yellow birch laminate	0.72	3.1	3.254	40.29	36.64	80.18
Yellow birch staypak laminate	1.30	4.7	3.406	37.88	65.34	106.63
Yellow birch impreg laminate	.86	33.2	4.648	35.11	37.05	76.81
Yellow birch compreg laminate	1.30	24.8	4.251	39.47	59.14	102.86
Do	1.31	34.3	4.931	39.32	54.83	99.08
Sitka spruce laminate	.53	26.0	3.837	37.14	27.67	68.65
Parallel-laminated papreg	1.40	36.5	5.73	15.14	65.10	85.97
Cross-banded papreg	1.40	36.5	10.89	[4]11.00	62.20	84.09
Molded hydrolyzed-wood plastic	1.33	25.	42.69	42.69	42.69	128.07
Hydrolyzed-wood sheet laminate	1.39	18.	13.49	24.68	77.41	115.58

[1] All wood laminates made from rotary-cut veneer, annual rings in plane of sheet.

[2] On basis of dry weight of product.

[3] Approximate.

[4] Calculated value.

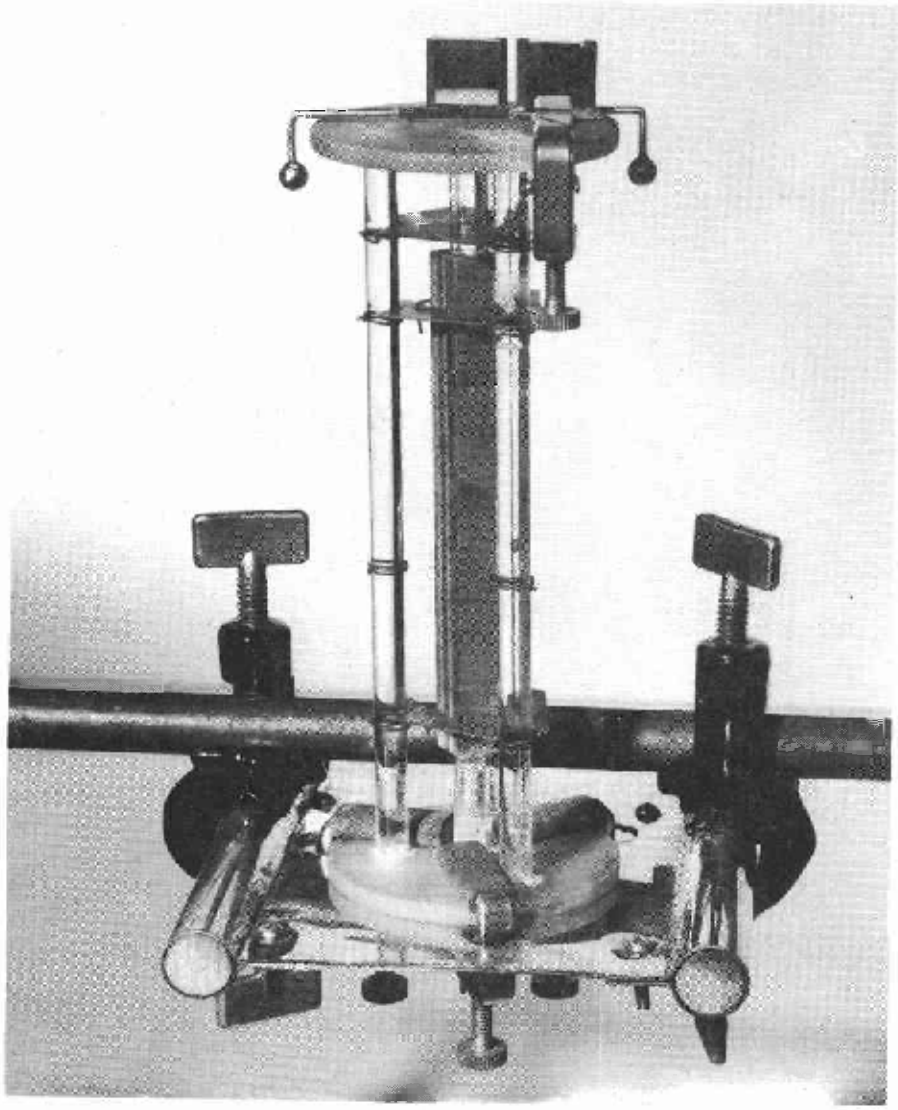

Figure 1.--Quartz dilatometer used in measuring the coefficient of linear expansion with a specimen in position for measurement in the fiber direction. Arms terminating in metal balls attached to the optical lever are to lower the center of gravity of the lever.

Z M 62942 F

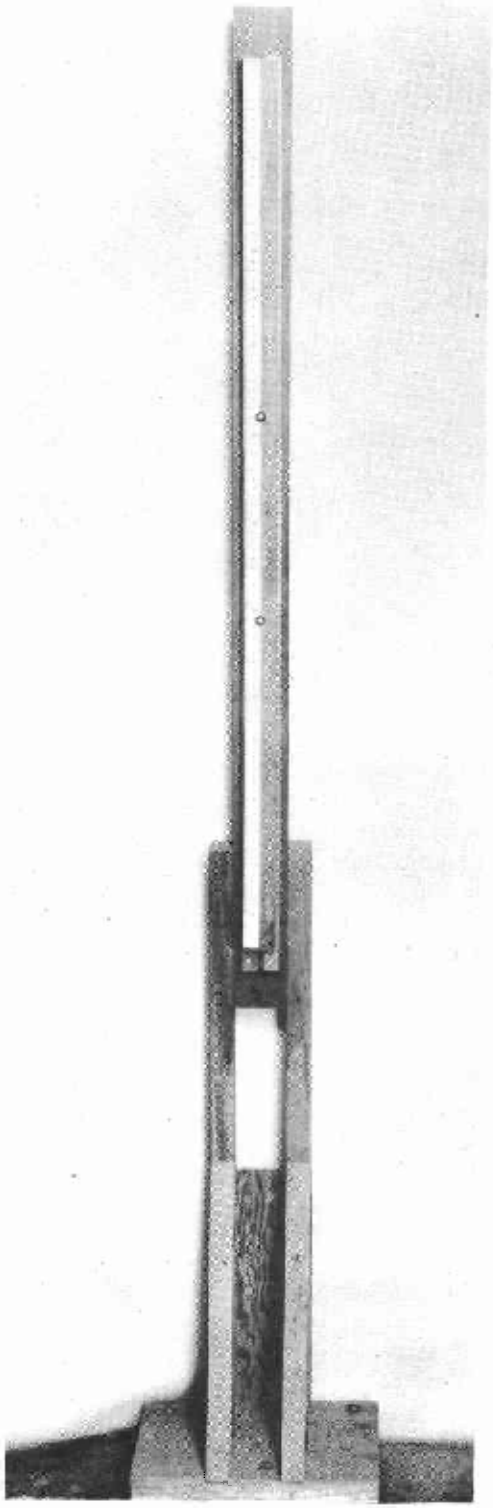

Figure 2.--Concave adjustable scale on which optical deflections are read.
Z M 62943 F

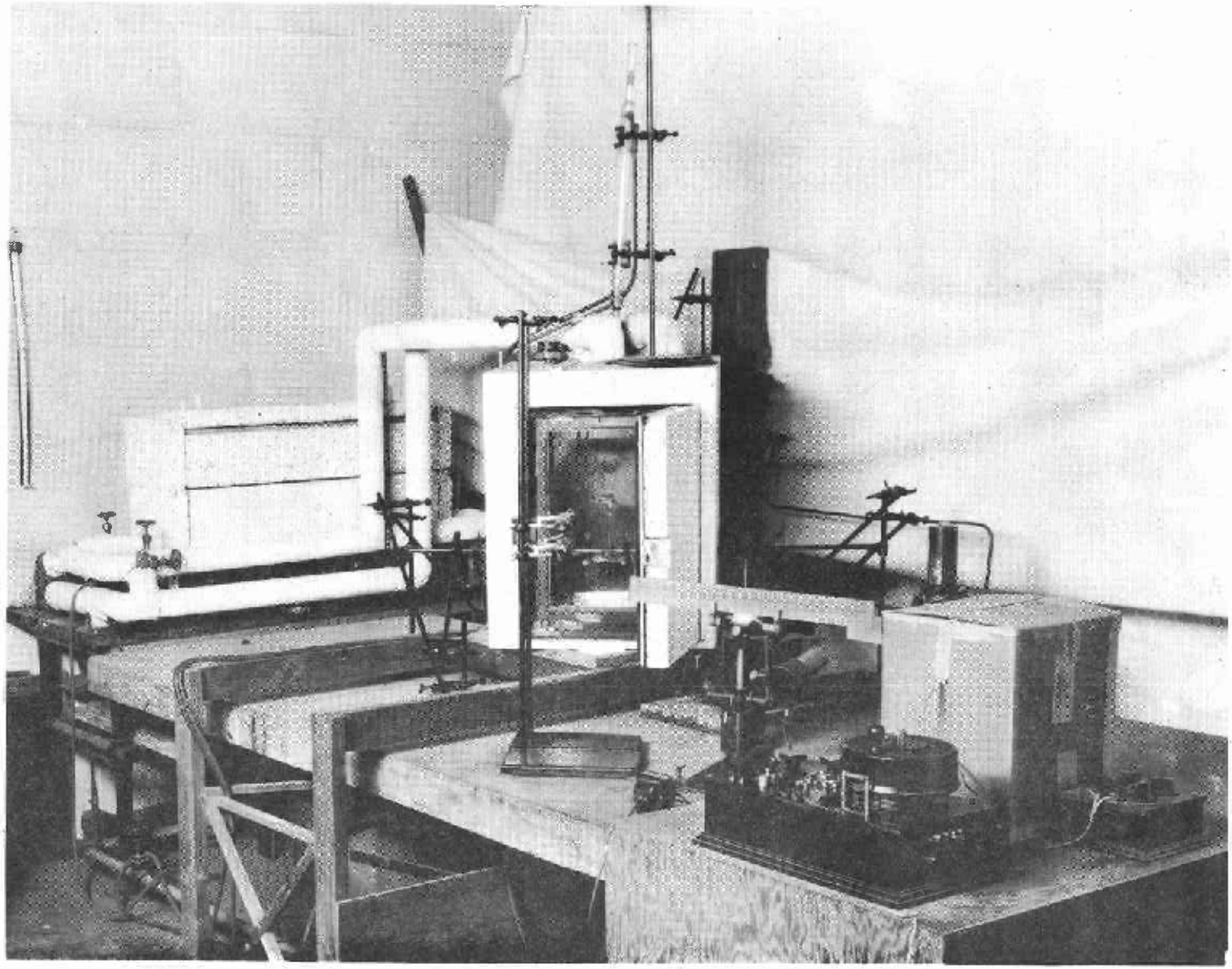

Figure 3.--Assembly used for measuring coefficients of linear thermal expansion, showing how the air bath containing the dilatometer is mounted free of the stone table on which the dilatometer is supported.

Z M 62944 F

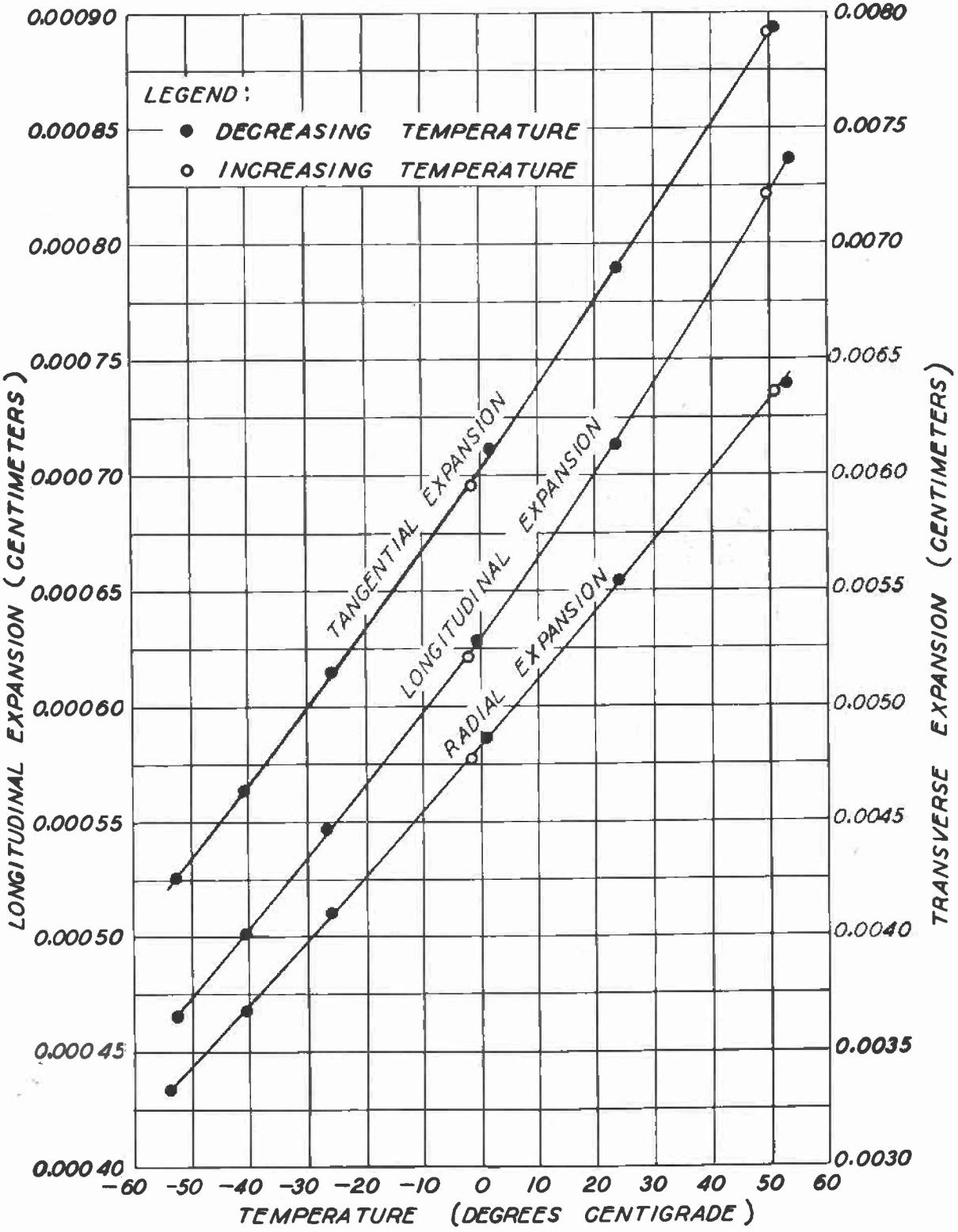

Figure 4.--Expansion of solid yellow-birch with a specific gravity, based on weight and volume when oven dry, of 0.593 between +50° and -55° C. in the three different structural directions.

Z M 62945 F

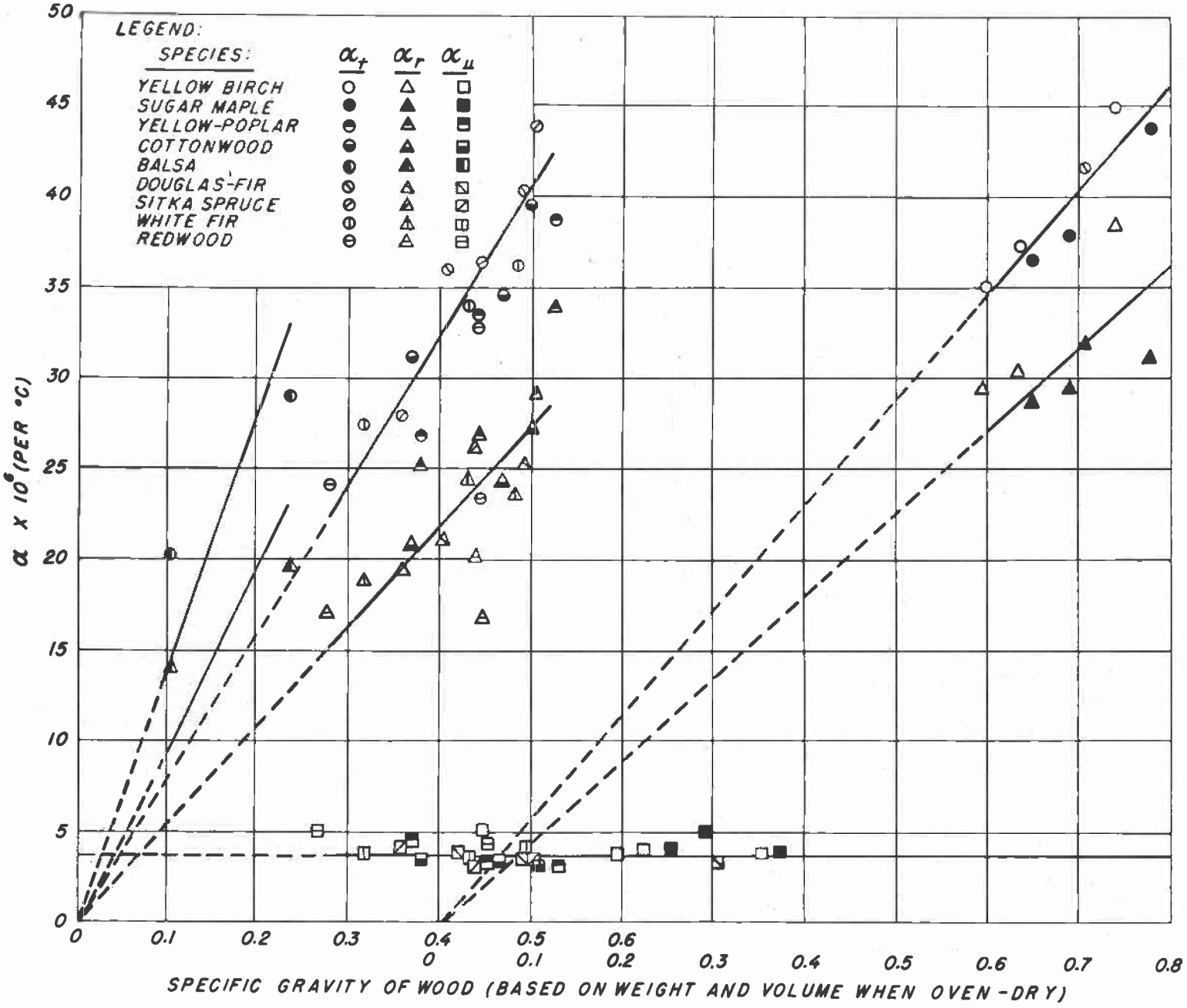

Figure 5.--Relationship of the coefficient of linear thermal expansion of nine species of natural wood between 0° and +50° C. in the three different structural directions to the specific gravity of the wood.

Z M 62946 F

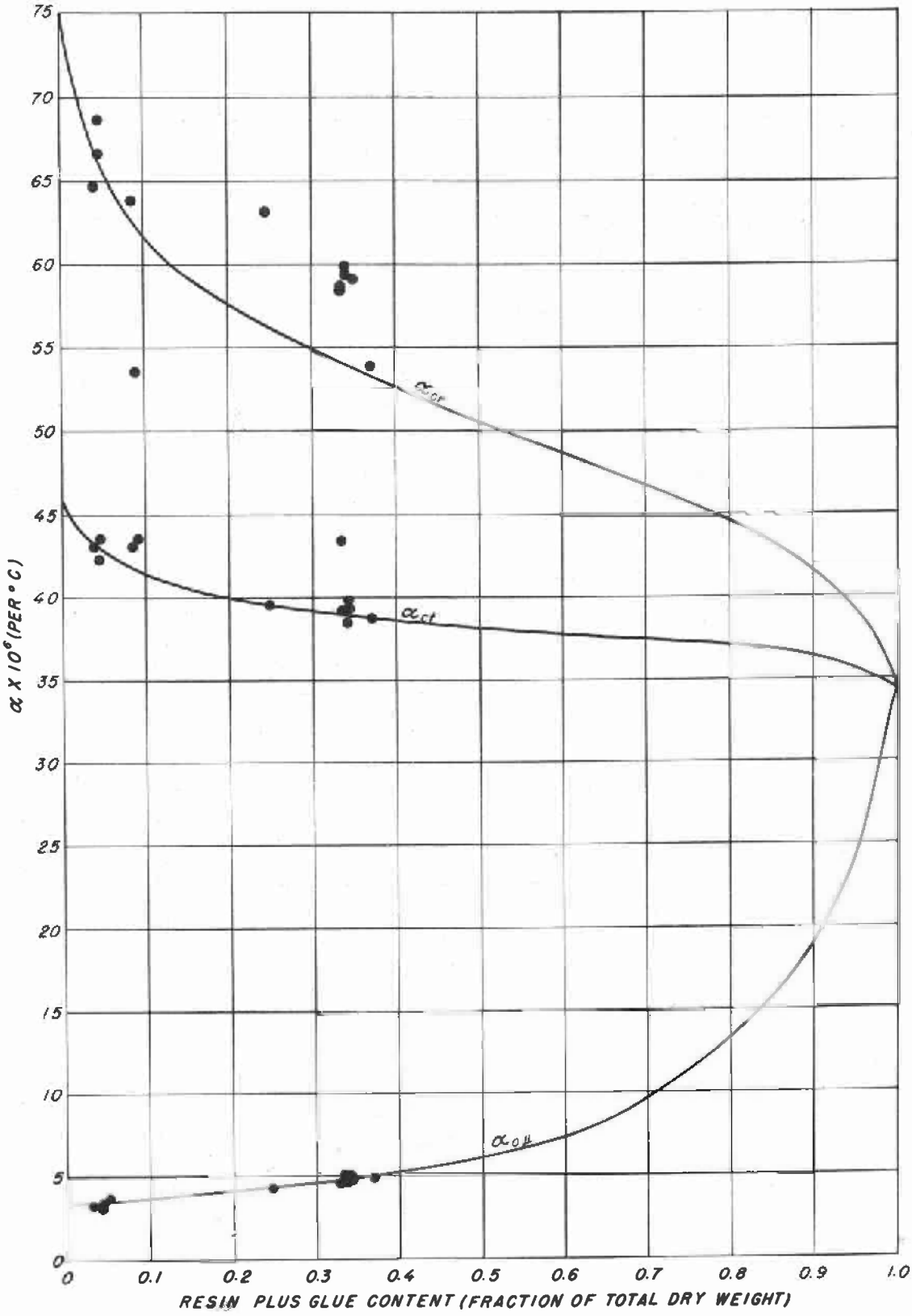

Figure 6.--Calculated curves for the coefficient of linear thermal expansion of compressed rotary-cut yellow-birch laminates with an original specific gravity of the wood of 0.6 and a final specific gravity of 1.2 versus the combined resin and glue content expressed as a fraction of the total dry weight, together with points for the observed values on specimens of different specific gravity taken from tables 3, 4, and 5.

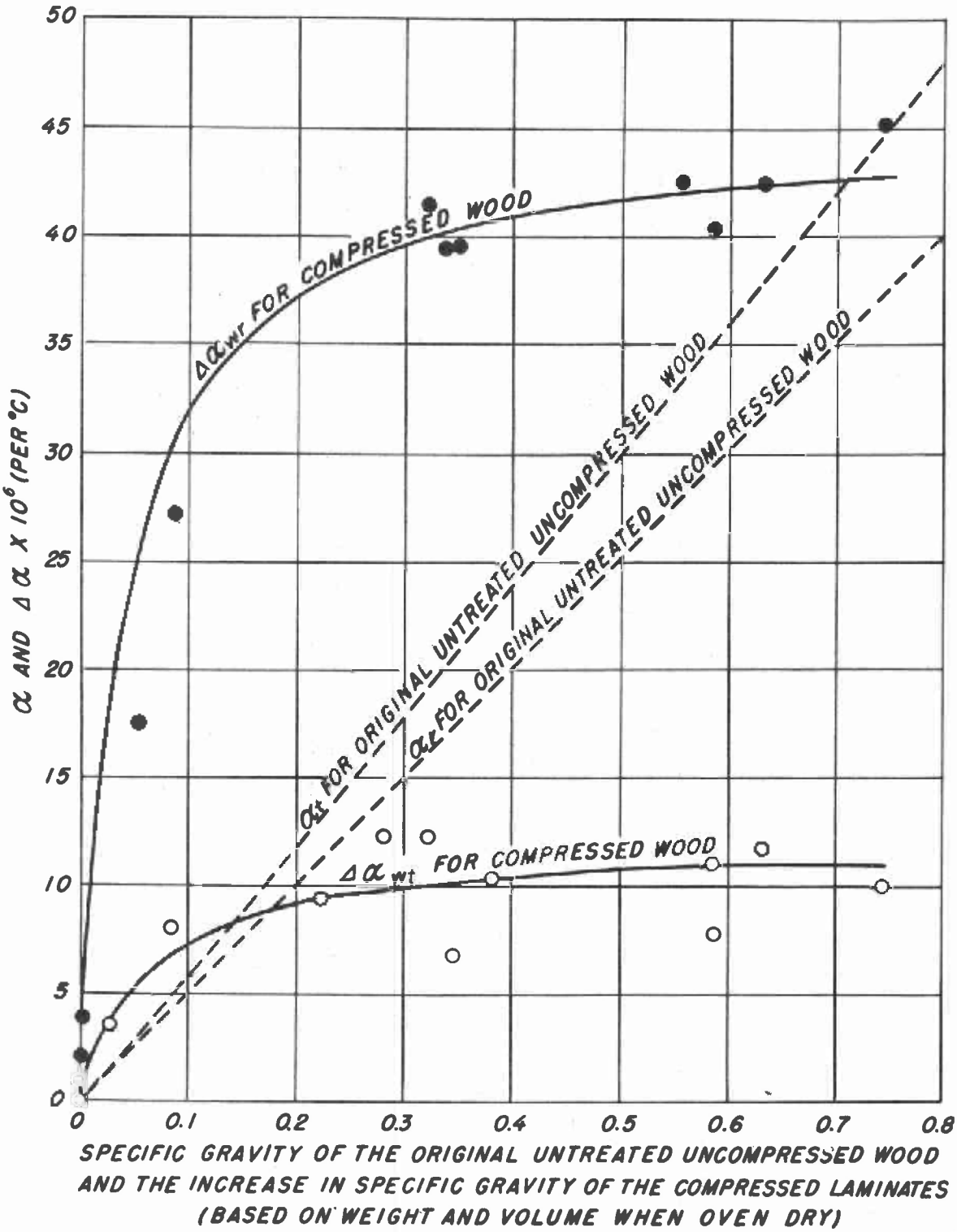

Figure 7.--Increase in the coefficients of linear thermal expansion of the wood portion of rotary cut yellow-birch laminates in the tangential and radial directions versus the specific gravity increase caused by radial compression, together with the increases in the coefficients of linear thermal expansion resulting from natural increases in specific gravity.

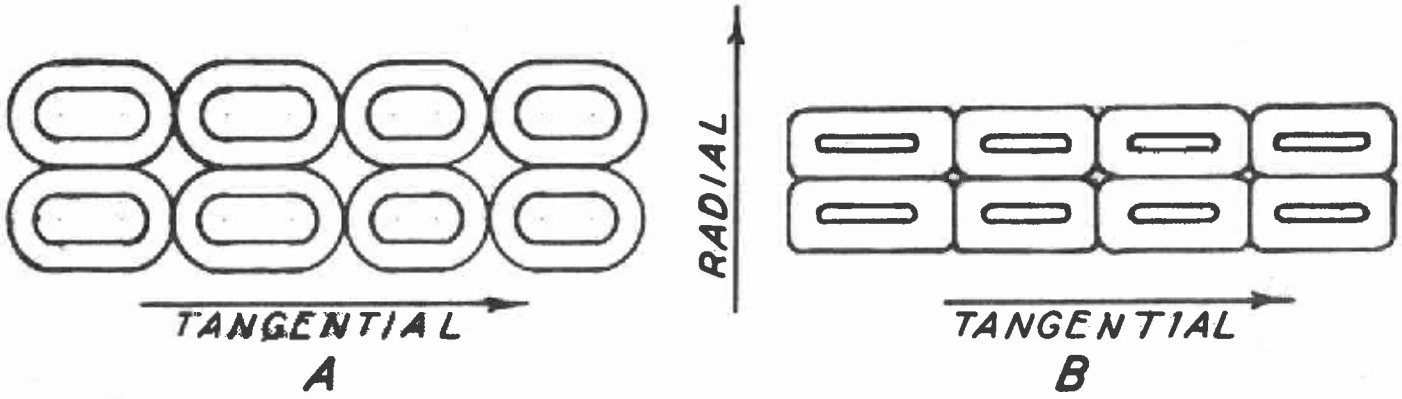

Figure 8.--Diagrammatic sketch of the cross section of wood fibers in (A) the uncompressed and (B) the compressed form.

Z M 62949 F

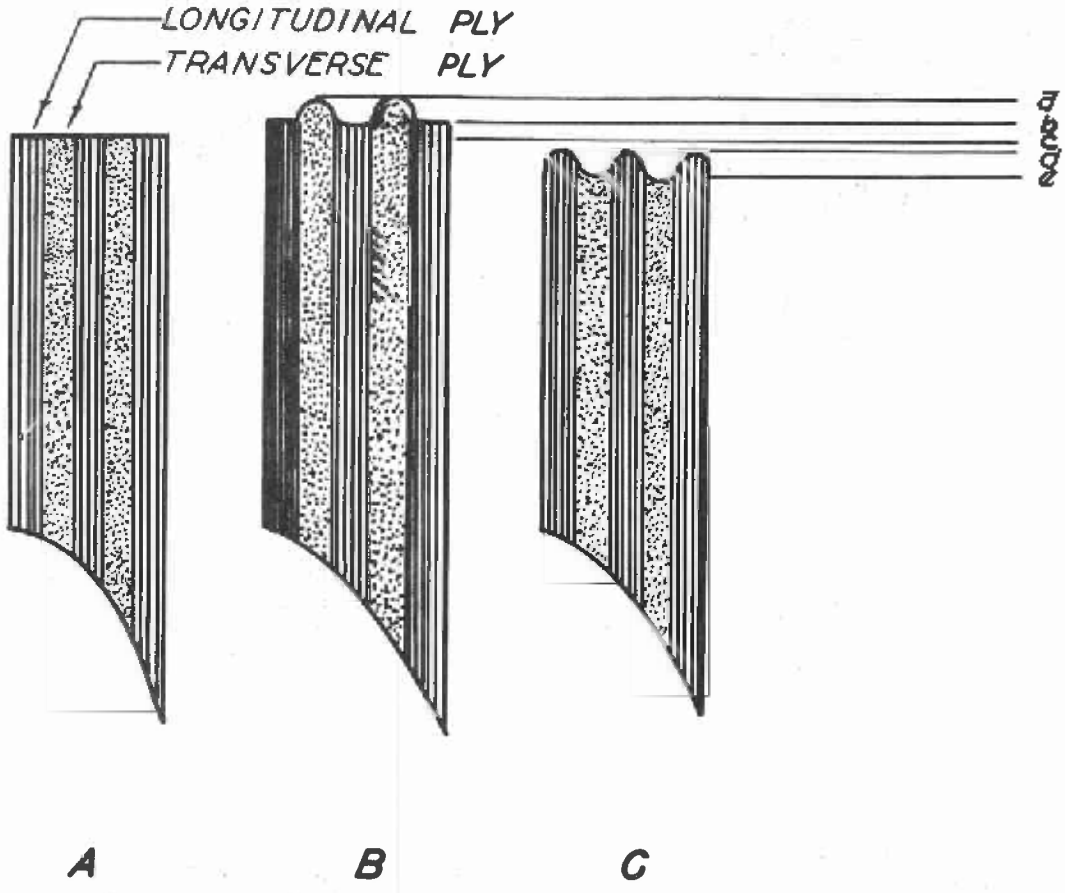

Figure 9.--Diagrammatic sketch of the edge washboarding of plywood due to different coefficients of linear thermal expansion in the two sheet directions, showing that the observed expansion ca and contraction ce exceeds the true expansion cb+ and true contraction cd+. A.--Held at cutting temperature. B.--Heated above cutting temperature. C.--Cooled below cutting temperature.

M 62950 F

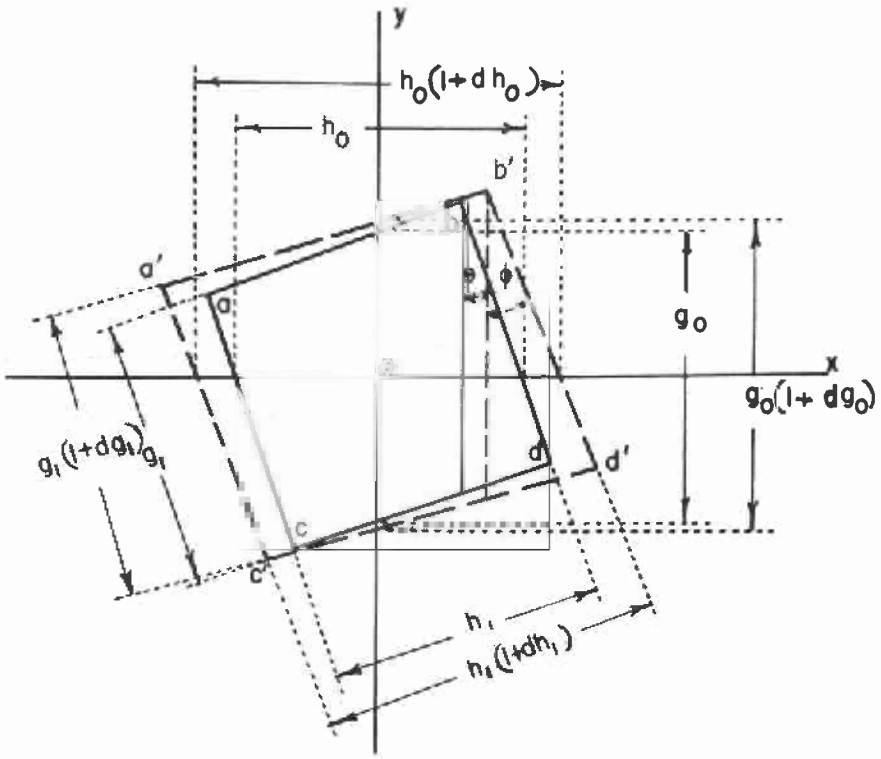

Figure 10.--Diagrammatic sketch of a rectangular plane of wood with grain angle θ before any thermal expansion (heavy solid line), and of the parallelogram (heavy dashed line), grain angle ϕ, resulting from the thermal expansions αh_o and αg_o.

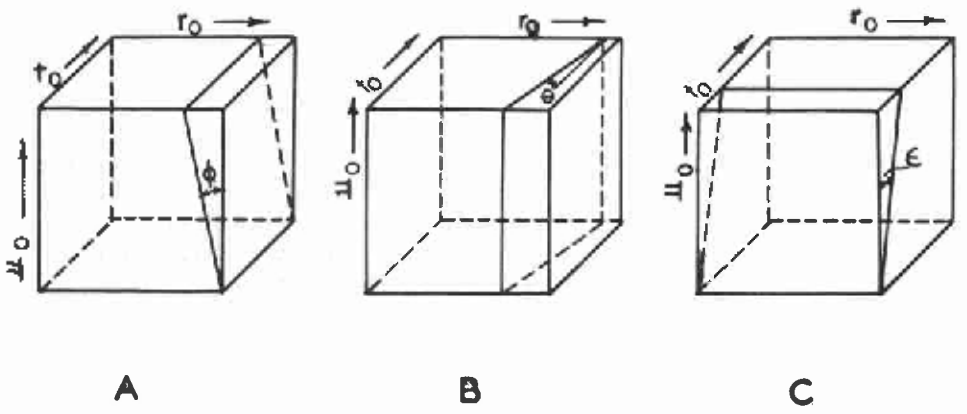

Figure 11.--Diagrammatic sketch of rectangular blocks of wood in which the grain makes an angle to only one of the faces of the block. (A) ϕ is the grain angle to the tangential plane, (B) θ the angle made by the slope of the annual rings to the tangential face, (C) ϵ the grain angle to the radial plane.

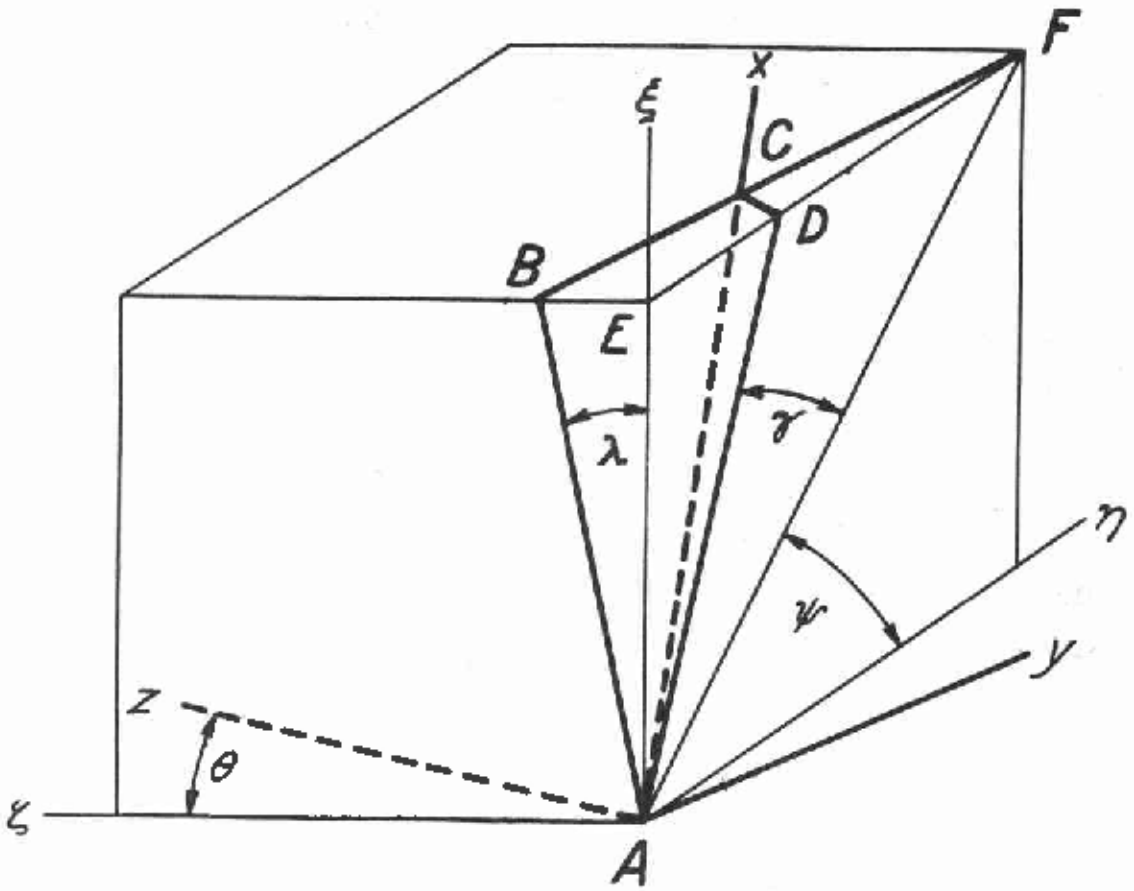

Figure 12.--Diagramatic sketch of a rectangular block of wood in which the line AC represents a wood fiber lying in the radial plane ACD and the tangential plane ACF. The ξ-, η-, and ζ-axes lie in the edges of the block, and the x-, y-, and z-axes are the natural axes of the wood. The angles λ, γ, and ψ, measured in the faces of the block, determine the direction-cosines of the two sets of axes with respect to each other.

M 68094 F

SUBJECT LISTS OF PUBLICATIONS ISSUED BY THE

FOREST PRODUCTS LABORATORY

The following list of publications are obtainable free on request from the Director, Forest Products Laboratory, Madison 5, Wis.:

Boxing and Crating

Building Construction

Chemistry of Wood and Derived Products

Fire Protection

Fungus Defects in Forest Products

Furniture Manufacture, Woodworkers and Teachers of Wood Shop Practice

Glue and Plywood

Growth, Structure, and Identification of Wood

Logging, Milling, and Utilization of Timber Products

Mechanical Properties of Wood

Pulp and Paper

Seasoning of Wood

Structural Sandwich, Plastic Laminates, and Wood-Base Aircraft Components

Wood Finish

Wood Preservation

Note: Since Forest Products Laboratory publications are so varied in subject no single list is issued. Instead a list is made up for each Laboratory division. Twice a year, December 31 and June 30, a list is made up showing new reports for the previous six months. This is the only item sent regularly to the Laboratory's mailing list. Anyone who has asked for and received the proper subject lists and who has had his name placed on the mailing list can keep up to date on Forest Products Laboratory publications. Each subject list carries descriptions of all other subject lists.